

Understanding the light curves of the HST-1 knot in M87 with internal relativistic shock waves along its jet

Y. Coronado¹, O. López-Corona^{1,2} & S. Mendoza^{1*}

¹ *Instituto de Astronomía, Universidad Nacional Autónoma de México, AP 70-264, Distrito Federal 04510, México*

² *Centro de Ciencias de la Complejidad, Universidad Nacional Autónoma de México, Ciudad Universitaria, Distrito Federal, México.*

ABSTRACT

Knots or blobs observed in astrophysical jets are commonly interpreted as shock waves moving along them. Long time observations of the HST-1 knot inside the jet of the galaxy M87 have produced detailed multi-wavelength light curves. In this article, we model these light curves using the semi-analytical approach developed by Mendoza et al. (2009). This model was developed to account for the light curves of working surfaces moving along relativistic jets. These working surfaces are generated by periodic oscillations of the injected flow velocity and mass ejection rates at the base of the jet. Using genetic algorithms to fit the parameters of the model, we are able to explain the outbursts observed in the light curves of the HST-1 knot with an accuracy greater than a 2- σ statistical confidence level.

Key words: hydrodynamics – relativistic processes – shock waves – galaxies:jets.

1 INTRODUCTION

The jet in the galaxy M87 was detected in the optical band by Curtis (1918). It is the closest Active Galaxy Nuclei with a redshift $z = 0.004360$ and has been extensively monitored in multi-frequency campaigns, particularly over the last decade. Radio interferometry and high resolution optical and X-ray observations show the complex structures formed inside the jet as close as ~ 100 pc from the nucleus (Waters & Zepf 2005). The most exotic of these structures, is a particular knot formed in 1999 and labelled HST-1. The evolution of HST-1 began to be closely followed in 2000 with the Chandra X-ray telescope (Harris et al. 2003, 2006, 2009) since it started to develop a rapid increase on its X-ray emission, achieving a maximum in 2005, corresponding to a factor of 50 as compared to the emission detected in 2000. After this maximum, the emission decreases and is followed by two further increments in 2006 and 2008. Ultraviolet (Madrid 2009) and radio (Chang et al. 2010) observations show a similar behaviour of its light curve. The whole emission of M87 presents an optical outburst in 2005 (Madrid 2009) which is related to the maximum emission of the HST-1 knot in the same year. This strongly suggests that the outburst is produced by the strong emission of the knot.

Knots in astrophysical jets are usually identified with internal shock waves travelling along the jet. These internal shock waves can be produced by different mechanisms: (a) interactions of the jet with an overdense medium, e.g. clouds (cf. Mendoza 2000; Mendoza & Longair 2001),

(b) bending of jets above a critical value (Mendoza 2000; Mendoza & Longair 2002), and (c) Periodic variations of the injected velocity and mass at the base of the jet (e.g. Rees & Meszaros 1994; Jamil et al. 2008; Mendoza et al. 2009, and references therein).

In the literature, the main contribution of the X-ray emission of the HST-1 knot is still under discussion and the interpretations vary between an effect of a hot accretion disc with the corona (Marscher et al. 2002) and a particular phenomena of a re-collimation shock (Stawarz et al. 2006), causing the impressive flare in X-rays. Later observations in radio revealed superluminal motions in HST-1 being a well isolated knot from the nucleus (Biretta et al. 1999), displaced from the central engine by ≥ 120 pc (Cheung et al. 2007). All this makes HST-1 the best studied knot for a possible internal shock mechanism inside a jet. It is also an ideal target to observe due to its proximity. The strong multi-wavelength emission from the jet and its knots allow to test the physics of knots and shock waves in the relativistic regime.

Since relativistic outbursts are usually thought of as internal shock waves travelling along the jet, produced by periodic variations of the injected flow, it is quite natural to model the high emission light curve of the HST-1 knot as shock waves produced by this mechanism. The semi-analytical model by Mendoza et al. (2009) (denoted as M09 in what follows) has been quite useful in modelling not only outbursts associated to long gamma-ray bursts but also to the many outbursts detected on the light curve of the blazar PKS 1510-089 (Cabrera et al. 2013). We show in this article, that such a model is also good for modelling and understand-

* E-mail address: {coronado,lopez,sergio}@astro.unam.mx.

ing the multi-frequency features observed in the HST-1 knot of the M87 galaxy.

Harris et al. (2009) found a quasi-periodic impulse signature in the brightening and dimming of the core of M87. This was interpreted as a manifestation of past modulation of jet power, possibly by a local oscillation of the process that converts the bulk kinetic jet power to the internal energy of the emitting plasma. This result reinforces the use of the M09 model in order to explain the formation and evolution of the HST-1 knot.

The article is organised as follows. In section 2 we present the multi-wavelength observation campaigns of the HST-1 knot and its light curves features. In section 3 we present a brief description of the hydrodynamical model developed by Mendoza et al. (2009) and the system of dimensionless units in which it is useful to make comparisons with observations. The fits to the light curves using the hydrodynamical model of Mendoza et al. (2009) are developed in the section 4. The result of our fits and a discussion of the obtained physical parameters of the model are presented in section 5.

2 OBSERVATIONAL DATA

The multi-frequency light curves were taken from three separate datasets and are shown in Figure 1. X-ray observations were taken from a multi-frequency program coordinating Chandra and HST monitoring (Harris et al. 2009). Ultraviolet data are part of the same program and carried out during the years 1999 to 2006 (Madrid 2009). Finally the radio data corresponds to observations with the VLBI at 2cm (Chang et al. 2010). As mentioned in section 1, these all show a clear outburst with a maximum emission occurring in 2005, followed by a small outburst. After this, subsequent micro-outbursts differ from each other in the global decay of the light curve. Although all the observational data show the same morphology in the light curves, the spectral power law differs in each section of the spectrum from radio to X-rays, revealing that a simple power law cannot describe the whole spectra of HST-1 (Harris et al. 2009).

We calculate the flux in X-rays following the procedure described by Harris et al. (2006) and applied it to the observational intensities of the HST-1 knot reported by Harris et al. (2009). The flux in ultraviolet and radio wavelengths is calculated with a conversion factor between Jy to W/m^2 , using a reference wavelength of 225.55nm for the ultraviolet data (Madrid 2009) and 2cm for the radio measurements (Chang et al. 2010).

We assume a negligible extinction factor and an isotropic emission of the source, located at a distance of 16Mpc corresponding to the distance to the galaxy M87 (Jordán et al. 2005). With these assumptions we obtain a lower limit for the luminosity of the HST-1 knot in different wavelengths.

3 MODEL

Let us assume that periodic injections of velocity and mass flows are injected at the base of a 1D relativistic flow moving along a jet and consider a particular time on the ejection

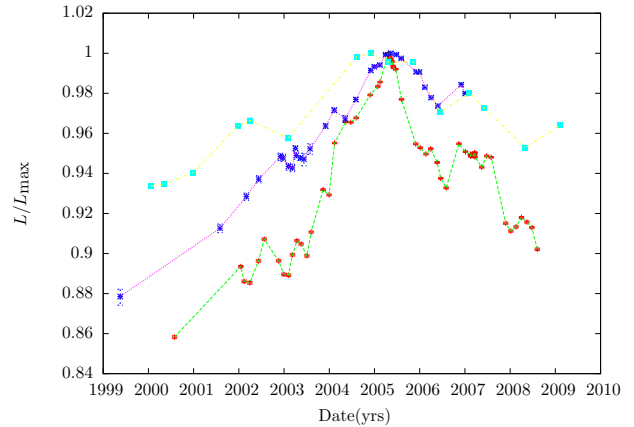


Figure 1. The figure shows multi-frequency luminosity curves of the HST-1 knot of the galaxy M87. All curves have been normalised to the maximum. From bottom to top, the curves represent 2cm radio (Chang et al. 2010), 225.5nm UV Madrid (2009) and Chandra 2Kev X-ray (Harris et al. 2009).

tion process in which a fast parcel of flow is ejected after a slow one. A time later, the fast parcel will “overtake” the slow one and the flow will become multi-valued. In order to arrange this contradiction, nature creates an initial discontinuity of the hydrodynamical values which later develops into a working surface, i.e. a contact discontinuity bounded by two shock waves, that moves along the jet on the direction of the flow as measured from the central engine (see e.g. Landau & Lifshitz 1995).

The first ideas about radiative internal shock waves inside an astrophysical jet were developed by Rees & Meszaros (1994); Daigne & Mochkovitch (1998). Although several extensions and particular aspects of the model have been presented in the literature (see e.g. Panaitescu et al. 1999; Spada et al. 2001; Sahayanathan & Misra 2005). A semi-analytical description of this phenomenon was made by M09. These last model assumes periodic injections of mass and velocity at the base of the jet. Using mass and conservations of the ejected material, it is possible to account for the kinetic power loss as the working surface travels along the jet, assuming that the radiation time scales are small compared to the characteristic dynamical times of the problem. The pressure of the fluid is thus negligible and so the description of the flow can be well described by a ballistic approximation. This assumption is valid if the flow within the jet is nearly adiabatic and non-turbulent (see e.g. Sahayanathan & Misra 2005). In what follows we will use the model by M09 to describe the multi-wavelength light curve features of the HST-1 knot in M87.

To follow the evolution of the working surfaces M09 considered a source ejecting material in a preferred direction with a velocity $v(\tau)$ and a mass ejection rate $\dot{m}(\tau)$, both dependent on the time τ as measured from the jet’s source. A further assumption is made such that the working surface is thin and mass losses within it are negligible. The energy loss E_r by the working surface is given by $E_r = E_0 - E_{ws}$, where E_0 is the injected energy at the base of the jet and E_{ws} is the energy inside the working surface. The kinetic power available within the working surface is then given by dE_r/dt . If this power is converted efficiently into radiated

energy then the Luminosity L produced by the emission of the working surface is given by $L = -dE_r/dt$.

On the one hand, we assume that the injected velocity at the base of the jet is a periodic function of time, given by:

$$v(\tau) = v_0 + c\eta^2 \sin(\omega\tau), \quad (1)$$

where the velocity v_0 is the “background” average bulk velocity of the flow inside the jet and ω is the oscillation frequency of the injected velocity. The positive dimensionless parameter η^2 measures the amplitude variations of the flow and is such that the oscillations of the flow are sufficiently small, in such a way that the total bulk velocity $v(\tau)$ does not exceeds the velocity of light c .

On the other hand, the mass ejection rate \dot{m} injected at the base of the jet has the following periodic variation:

$$\dot{m} = \dot{m}_0 + \dot{\mu} \sin(\Omega\tau). \quad (2)$$

where \dot{m}_0 is the “background” average mass ejection rate and Ω is the oscillation frequency of the mass ejection rate. The parameter $\dot{\mu}$ is the amplitude of the injected oscillation.

In the original article by M09 and in further applications (see e.g. Cabrera et al. 2013; Coronado & Mendoza 2014) the modelling of outbursts for long gamma-ray bursts, blazars and micro-quasars was performed under the assumption that $\dot{\mu} = 0$ and so $\dot{m} = \text{const}$. Although this simplifies the number of free parameters of the model, it turns out that the light curve of the HST-1 knot in M87 cannot be modelled with such a simple assumption.

In order to use the semi-analytical ballistic M09 model on its more general form, we proceed as follows. The model depends on six unknown parameters: v_0 , η^2 , ω , \dot{m}_0 , $\dot{\mu}$, and Ω . To reduce the number of unknown parameters, we proceed as follows.

The luminosity L depends on six dimensional parameters: v_0 , $c\eta^2$, ω , \dot{m}_0 , $\dot{\mu}$, and Ω . Additionally, the velocity of light c is an important dimensional parameter of the relativistic phenomena we are dealing with and so, it has to be added to the list of important dimensional quantities of the problem. Since there are three fundamental independent dimensions, namely the dimensions of time, length and mass, Buckingham’s Π -Theorem of dimensional analysis means that the luminosity can be described as follows:

$$L = \dot{m}_0 c^2 L' (v_0/c, \eta^2, \dot{\mu}/\dot{m}_0, \Omega/\omega). \quad (3)$$

In the previous equation, the dimensionless luminosity L' is a function of the four dimensionless quantities v_0/c , η^2 , $\dot{\mu}/\dot{m}_0$, Ω/ω . In other words, the seven dimensional quantities for which the luminosity depends on, can be reduced to the problem of only four dimensionless quantities.

4 FITS TO THE OBSERVATIONAL DATA

The observed and theoretical luminosities, L_{obs} and L_{th} respectively, can be fit to the observational data with the use

of their dimensionless counterparts L'_{obs} and L'_{th} by rescaling them as follows. Both theoretical and observed dimensionless luminosities can be normalised to their maximum values: $L'_{\text{obs}}(\tau'_{\text{max}})$ and $L'_{\text{th}}(\tau'_{\text{max}})$, i.e.

$$\mathbb{L}_{\text{obs}} := \frac{L'_{\text{obs}}}{L'_{\text{obs}}(\tau'_{\text{obs,max}})}, \quad \mathbb{L}_{\text{th}} := \frac{L'_{\text{th}}}{L'_{\text{th}}(\tau'_{\text{th,max}})}, \quad (4)$$

where the dimensionless times $\tau'_{\text{obs,max}}$ and $\tau'_{\text{th,max}}$ correspond to the particular times where the observed or theoretical luminosities reach a maximum value respectively. According to Buckingham’s Π -Theorem of dimensional analysis, the dimensionless time τ' is related to the time τ by the following relation:

$$\tau = \omega^{-1} \tau'. \quad (5)$$

In order to measure the observed and theoretical times in the same system of dimensionless units we normalised them to the time given by the FWHM of the outburst, i.e.:

$$\mathbb{T}_{\text{obs}} := \frac{\tau'_{\text{obs}}}{\tau'_{\text{obs}}(\text{FWHM})}, \quad \mathbb{T}_{\text{th}} := \frac{\tau'_{\text{th}}}{\tau'_{\text{th}}(\text{FWHM})}. \quad (6)$$

The best fit of the theoretical luminosity $\mathbb{L}_{\text{th}}(\mathbb{T}_{\text{th}})$ to the observed light curve $\mathbb{L}_{\text{obs}}(\mathbb{T}_{\text{obs}})$ yields a direct best value for the four dimensionless free parameters v_0/c , η^2 , $\dot{\mu}/\dot{m}_0$, Ω/ω . The quantity \dot{m}_0 is obtained by using (3) evaluated at one particular point of the light curve, which we choose as the point where the light curve reaches its maximum value. Once this last quantity is known, the value for the parameter $\dot{\mu}$ is hence inferred. The frequency ω is obtained using equation (5) evaluated at a particular time, which we choose as the time where the light curve reaches its maximum value. With this, the parameter Ω is then inferred.

The parameter calibration of the model is conceptualised as an optimisation problem and so, we propose to solve it using Genetic Algorithms (GAs), which are evolutionary based stochastic search algorithms that mimics natural evolution. In this heuristic search technique, points in the search space are considered as individuals (solution candidates), which as a whole form a population. The particular fitness of an individual is a number, indicating its quality for the problem at hand. As in nature, GAs include a set of fundamental genetic operations that work on the genotype, i.e. the solution candidate codification, namely: mutation, recombination and selection operators Mitchell (1998). These algorithms operate with a population of individuals $P(t) = x_1^t, \dots, x_N^t$, for a particular t iteration, where the fitness of each x_i individual is evaluated according to a set of objective functions $f_j(x_i)$. This objectives functions allows to order from best to worst individuals of the population in a continuum of degrees of adaptation. Individuals with higher fitness, recombine their genotypes to form the gene pool of the next generation, in which random mutations are also introduced to produce a new variability.

A fundamental advantage of GAs versus traditional methods is that GAs solve discrete, non-convex, discontinuous, and non-smooth problems successfully and so, they have been widely used in Ecology, Natural Resources Management, among other fields (López-Corona et al.

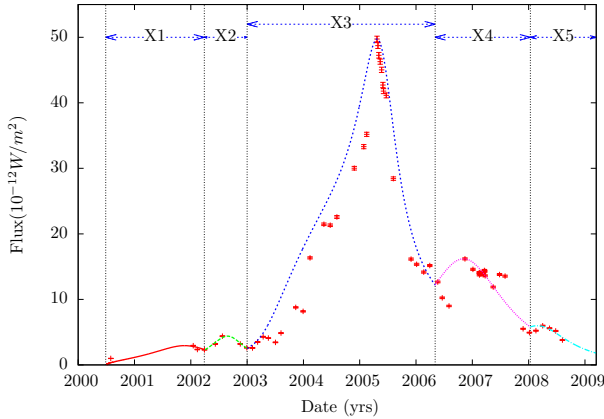


Figure 2. The figure show the fits (lines) to the X-ray data points of the light curve of the HST-1 knot observed by Harris et al. (2009) using the model by M09. The data points were divided into 5 time sections marked by the dotted vertical lines corresponding to individual outbursts, and labelled X1, X2, X3, X4 and X5. The resulting calibration of the free parameters of the model by M09 to the observed light curve are shown in Table 1.

2013) with some astrophysical applications (see e.g. Feigelson & Babu 2012). Our GA evaluated the luminosity function $\mathbb{L}_{\text{th}}(v_0/c, \eta^2, \dot{\mu}/\dot{m}_0, \Omega/\omega)$ of M09 in order to compare numerical results from the model with the observed light curve \mathbb{L}_{obs} using standard Residual Sum of Squares (RSS) as objective functions. All parameters were searched in the broadest possible range: $0.1 \lesssim v_0/c \lesssim 0.999$, $0.0001 \lesssim \eta^2 \lesssim 0.899$, $0.001 \lesssim \dot{\mu}/\dot{m}_0 \lesssim 1.0$ and $0.001 \lesssim \Omega/\omega \lesssim 20$. The choice is consistent with the physical restriction of keeping subluminal the full bulk velocity of the flow v and to the fact that a large value of $\dot{\mu}/\dot{m}_0$ would yield a huge unphysical luminosity value. A very large value of Ω/ω produces large mass ejection oscillations, something not clearly visible from the light curves. This search parameter technique generates populations of 100 possible solutions over a maximum 5000 generation search process, with a total of 500000 individuals. The GA algorithms selected were: tournament selection with replacement (Goldberg et al. 1989; Sastry & Goldberg 2001), simulated binary crossover (SBX) (Deb & Kumar 1995) and polynomial mutation (Deb & Kumar 1995; Deb 2001). The obtained final parameters were estimated by averaging the 500 best individuals.

Direct inspection of the light curves in Figure 1 show that multiple outbursts occur during the period of observation. As such and following the procedure of Cabrera et al. (2013) we divided the light curves into individual outbursts. Two clear outbursts appear on all wavelength observations and an additional 3 mini-outburst were defined for the X-ray data -two before the main outburst and one at the end of the observations. The results of the GA explained above for each outburst are presented in Table 1 and the best fits to the light curves with these parameters are shown in Figures 2-4.

5 DISCUSSION

Every modelling process goes an initial exploratory face in which a basic hypothesis space is set up. In this context, Williams (2014) found that a good modelling process should:

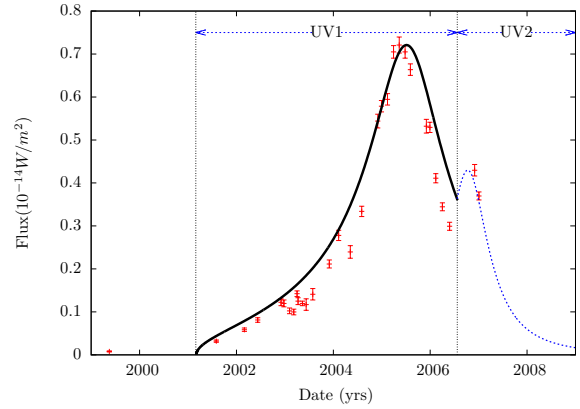


Figure 3. The figure show fits (lines) to the UV data points of the light curve of the HST-1 knot observed by Madrid (2009) using the model by M09. The data points were divided into 2 time sections marked by the dotted vertical lines corresponding to individual outbursts, and labelled UV1 and UV2. The resulting calibration of the free parameters of the model by M09 to the observed light curve are shown in Table 1.

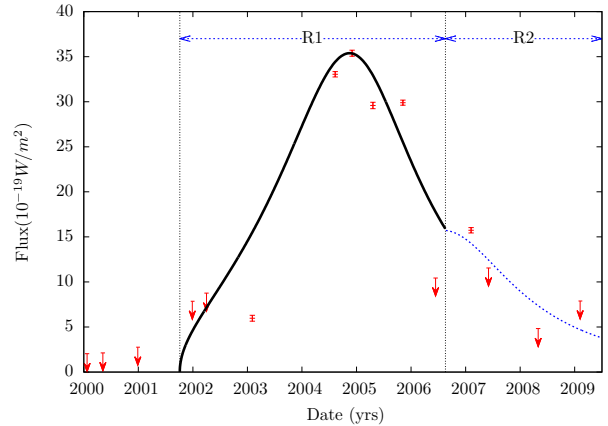


Figure 4. The figure show fits (lines) to the radio data points of the light curve of the HST-1 knot observed by Chang et al. (2010) using the model by M09. The data points were divided into 2 time sections marked by the dotted vertical lines corresponding to individual outbursts, and labelled R1 and R2. The resulting calibration of the free parameters of the model by M09 to the observed light curve are shown in Table 1.

(a) stay as close as data as possible, (b) includes as much phenomenological information as possible and (c) keep as simple as possible.

The parameter estimation of the model is quite close to the observational data (since it has a $\gtrsim 2\sigma$ confidence level value), with a simple ballistic model describing a complicated hydrodynamical phenomenon.

At first sight, the curves seem not to properly adjust to many data points, as one should expect with such small observational uncertainties in the data. However, the time series represented by the light curve has many temporal gaps. Between these temporal gaps, the value of the inferred physical parameters may not stay the same, making the light curve to present mini-outbursts combined with different oscillations. For example, the data points about 2007 in X-rays

ID	v_0/c	η^2	\dot{m}_0 ($10^{-3}M_\odot\text{yr}^{-1}$)	$\dot{\mu}$ ($10^{-3}M_\odot\text{yr}^{-1}$)	\dot{m}_{max} ($10^{-3}M_\odot\text{yr}^{-1}$)	ω_0^{-1} (days)	Ω^{-1} (days)	Γ_{min}	Γ_{max}	Γ_{bulk}
X ₁	0.9631	0.0360	4.252	0.415	4.667	53.8	0.716	2.67	23.12	3.72
X ₂	0.9573	0.0420	3.476	1.119	4.596	26.4	4.361	2.48	27.32	3.46
X ₃	0.8156	0.1839	9.727	3.943	13.671	374	2322.5	1.29	31.32	1.73
X ₄	0.9713	0.0275	36.56	3.351	39.916	118	45.874	3.03	20.16	4.2
X ₅	0.9150	0.0823	4.511	2.057	6.569	83.5	36.0	1.81	13.49	2.48
			($10^{-6}M_\odot\text{yr}^{-1}$)	($10^{-6}M_\odot\text{yr}^{-1}$)	($10^{-6}M_\odot\text{yr}^{-1}$)					
UV ₁	0.9020	0.0976	1.569	0.588	2.157	296	50.818	1.68	32.97	2.32
UV ₂	0.9762	0.0228	8.094	3.338	11.433	16.1	4.139	3.31	22.83	4.61
			($10^{-9}M_\odot\text{yr}^{-1}$)	($10^{-9}M_\odot\text{yr}^{-1}$)	($10^{-9}M_\odot\text{yr}^{-1}$)					
R ₁	0.9450	0.0536	2.650	2.033	4.683	195.5	33.072	2.21	19.18	3.06
R ₂	0.9724	0.0270	9.156	2.821	11.978	75.43	31.21	3.07	27.12	4.28

Table 1. Best parameter estimations using the X-ray, UV and radio light curves of the HST-1 knot of the galaxy M87. The resulting light curves are shown in Figures 2-4. The fits were performed by dividing the light curves in time ID sections represented by the first column of the table. The quantity \dot{m}_{max} corresponds to the maximum mass ejection rate discharged by the jet for a particular outburst. The values Γ_{min} , Γ_{max} and Γ_{bulk} are the minimum, maximum and background (i.e. v_0 bulk “average” velocity of the flow) Lorentz factors of the flow. All parameters were obtained to a precision above a $2\text{-}\sigma$ statistical confidence level.

can be modelled as a series of mini-outbursts. But modelling such a number of mini-bursts in a context of insufficient physical data represents an increase of unjustified additional hypothesis, despite the fact of an increment in statistical accuracy. As pointed out by Roos & Rakos (2000) it should be expected some sort of conflict between parsimony and realism. Nevertheless as models tends to incorporate more hypothesis, and become increasingly complex there is lose in transparency interpretation.

Although equation (3) is dimensionally correct it doesn’t take into account the fact that an efficiency proportionality factor ξ should appear in the right hand side of the equation, i.e. $L = \xi\dot{m}_0c^2L'$. This factor does not only depend on the ratio of the radiated luminosity to kinetic loss power inside the working surface, but also on the frequency of the emitted radiation. This is the reason as to why the inferred mass ejection rates for the same outburst differ so much at different wave-lengths. In other words, at best one should consider the values of the mass ejection rates in Table 1 as lower limits. The inferred Lorentz factors for the bulk flow are $\sim 1 - 4$ reaching maximum values of up to ~ 30 .

The model by M09 has shown to be quite useful reproducing light curves of long gamma-ray bursts, blazars and micro-quasars. As we have shown in this article, the same model is also good for dealing with the light curve of the HST-1 knot of M87. Our modelling can be adjust more precisely to the observed data by suitably performing more subdivisions of the data set, essentially modelling many mini-outburst. Since no data is available for these mini-outbursts, their introduction would be speculative. In this sense, the current modelling can be interpreted as a baseline modelling (Schwab & Starbuck 2013) that captures the key patterns in the empirical data and the associated physical processes.

ACKNOWLEDGMENTS

This work was supported by DGAPA-UNAM (IN111513-3) and CONACyT (240512) grants. YC, OL and SM acknowledge economic support from CONACyT (210965, 62929 and 26344). OL acknowledges economic support from a DGAPA-UNAM fellowship.

References

- Biretta J. A., Sparks W. B., Macchetto F., 1999, ApJ, 520, 621
- Cabrera J. I., Coronado Y., Benítez E., Mendoza S., Hiriart D., Sorcia M., 2013, MNRAS, 434, L6
- Chang C. S., Ros E., Kovalev Y. Y., Lister M. L., 2010, *ap*, 515, A38+
- Cheung C. C., Harris D. E., Stawarz L., 2007, ApJL, 663, L65
- Coronado Y., Mendoza S., 2014, arXiv:1401.5395
- Curtis H. D., 1918, Publications of Lick Observatory, 13, 55
- Daigne F., Mochkovitch R., 1998, MNRAS, 296, 275
- Deb K., 2001, Multi-objective optimization using evolutionary algorithms. Vol. 16, John Wiley & Sons
- Deb K., Kumar A., 1995, Complex systems, 9, 431
- Feigelson E., Babu G., 2012, Modern Statistical Methods for Astronomy: With R Applications. Cambridge University Press
- Goldberg D. E., Korb B., Deb K., 1989, Complex systems, 3, 493
- Harris D. E., Biretta J. A., Junor W., Perlman E. S., Sparks W. B., Wilson A. S., 2003, ApJL, 586, L41
- Harris D. E., Cheung C. C., Biretta J. A., Sparks W. B.,

- Junor W., Perlman E. S., Wilson A. S., 2006, *ApJ*, 640, 211
- Harris D. E., Cheung C. C., Stawarz L., Biretta J. A., Perlman E. S., 2009, *ApJ*, 699, 305
- Jamil O., Fender R. P., Kaiser C. R., 2008, in *Microquasars and Beyond Internal Shocks Model for Microquasar Jets*
- Jordán A., Côté P., Blakeslee J. P., Ferrarese L., McLaughlin D. E., Mei S., Peng E. W., Tonry J. L., Merritt D., Milosavljević M., Sarazin C. L., Sivakoff G. R., West M. J., 2005, *ApJ*, 634, 1002
- Landau L., Lifshitz E., 1995, *Fluid Mechanics*, 2nd ed. edn. Vol. 2 of *Course of Theoretical Physics*, Pergamon
- López-Corona O., Padilla P., Escolero O., Armas F., Garca-Arrazola R., Esparza R., 2013, *Complexity*, 19, 9
- Madrid J. P., 2009, *Astronomical Journal*, 137, 3864
- Marscher A. P., Jorstad S. G., Gómez J., Aller M. F., Teräsranta H., Lister M. L., Stirling A. M., 2002, *Nature*, 417, 625
- Mendoza S., 2000, PhD thesis, Cavendish Laboratory, Cambridge University U.K., available at <http://www.mendozza.org/sergio/phdthesis>
- Mendoza S., Hidalgo J. C., Olvera D., Cabrera J. I., 2009, *MNRAS*, 395, 1403
- Mendoza S., Longair M. S., 2001, *MNRAS*, 324, 149
- Mendoza S., Longair M. S., 2002, *MNRAS*, 331, 323
- Mitchell M., 1998, *An Introduction to Genetic Algorithms*. A Bradford book, Bradford Books
- Panaiteescu A., Spada M., Mészáros P., 1999, *ApJL*, 522, L105
- Rees M. J., Meszaros P., 1994, *ApJL*, 430, L93
- Roos A., Rakos C., 2000, *Biomass and Bioenergy*, 18, 331
- Sahayanathan S., Misra R., 2005, *ApJ*, 628, 611
- Sastry K., Goldberg D. E., 2001, *Intelligent Engineering Systems Through Artificial Neural Networks*, 11, 129
- Schwab A., Starbuck W. H., 2013, *Philosophy of Science and Meta-Knowledge in International Business and Management*, 26, 171
- Spada M., Ghisellini G., Lazzati D., Celotti A., 2001, *MNRAS*, 325, 1559
- Stawarz L., Aharonian F., Kataoka J., Ostrowski M., Siemiginowska A., Sikora M., 2006, *MNRAS*, 370, 981
- Waters C. Z., Zepf S. E., 2005, *ApJ*, 624, 656
- Williams B. G., 2014, arXiv preprint arXiv:1412.2788